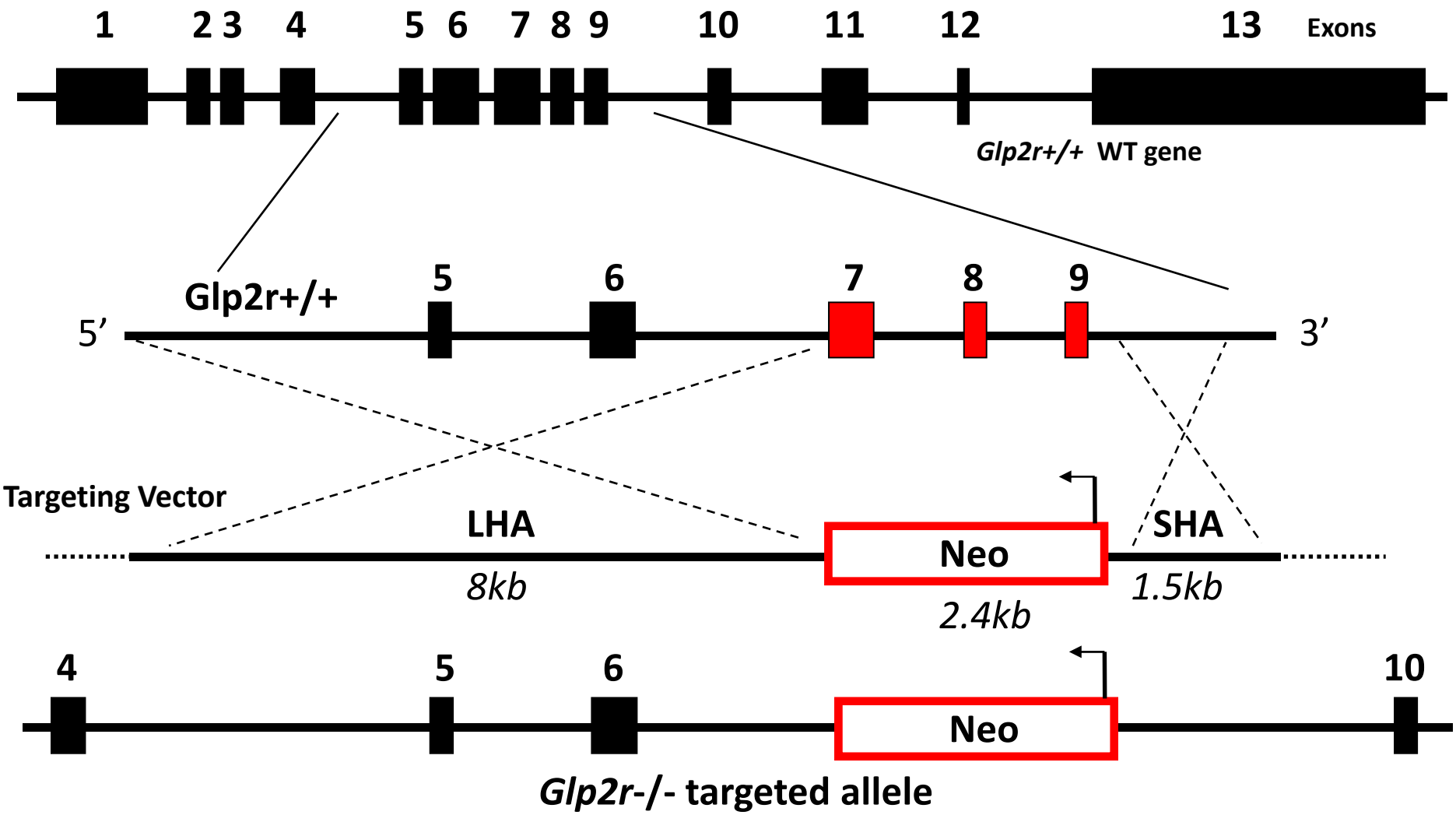

Supplementary Figure 1. *Targeting strategy for disruption of the Glp2r gene*. Exons 7-9 in the *Glp2r* gene were replaced by the Long Homology Arm (LHA), the Short Homology Arm (SHA) and the neomycin (Neo) resistance cassette as shown.

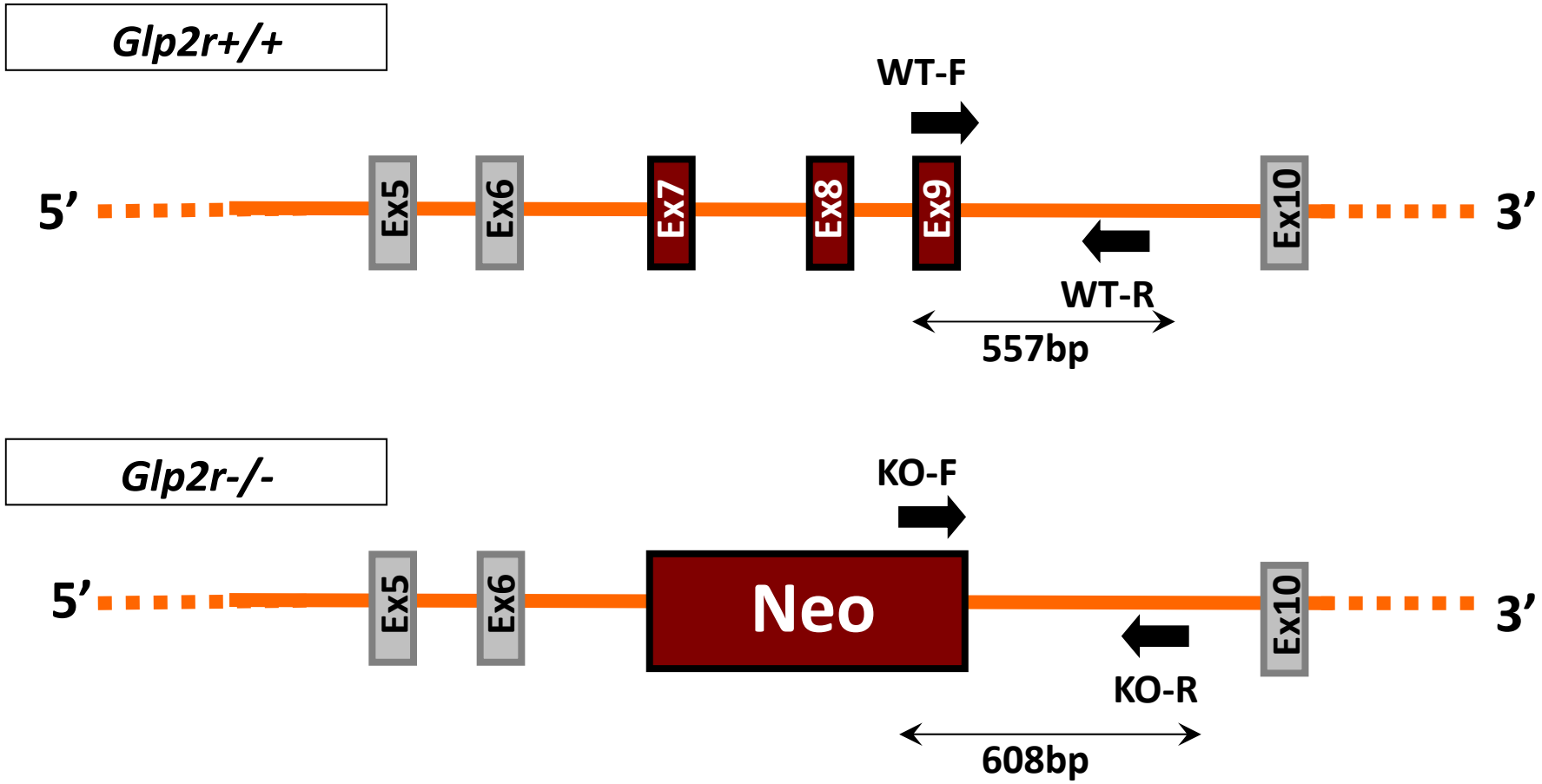

Supplementary Figure 2. *Genotyping of Glp2r-/- mice using the polymerase chain reaction*. Exons 5-10 of the *Glp2r* gene are shown. In the *Glp2r-/-* mice, the neomycin cassette replaces 2.45 kilobase of the *Glp2r+/+* gene, including exons 7-9. The sizes of the PCR products for Wildtype (WT) and knockout (KO) mice are indicated in number of base pairs. The wide solid arrows indicate the locations of the primers. Sequences of the primers are as follows:
WT-F (*Glp2r+/+* forward): 5'-TGCTGGGCAGTAAATGAGAA-3'
WT-R (*Glp2r+/+* reverse): 5'-CCCCACTTGCTGATGACATT-3'
KO-F (*Glp2r-/-* forward): 5'-TGCGAGGCCAGAGGCCACTTGTGTAGC-3'
KO-R *(Glp2r-/-* reverse)*:* 5'-ATCTCTTCCATTGCCCATGA-3'

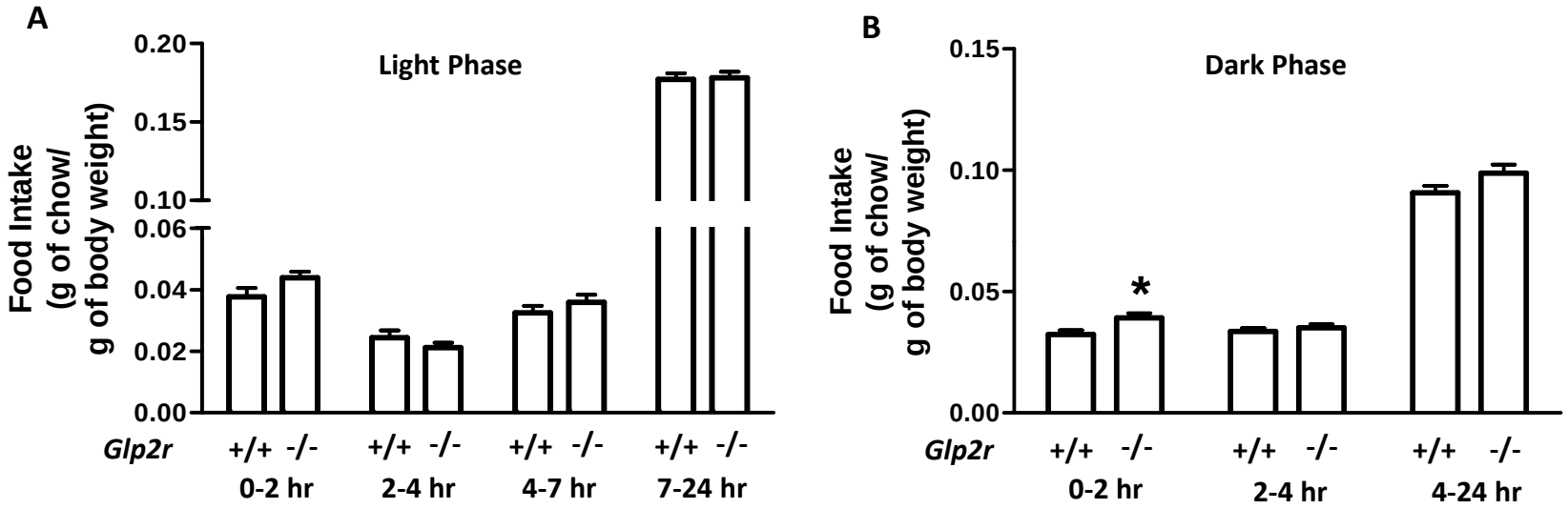

Supplementary Figure 3. Basal food intake assessed during (A) light and (B) dark phase periods following 12h (light phase) or 16 h (dark phase) of food deprivation in male *Glp2r*+/+ vs. *Glp2r*-/- mice. n=16 per group. *P<0.05 for *Glp2r*-/- vs *Glp2r*+/+ mice.

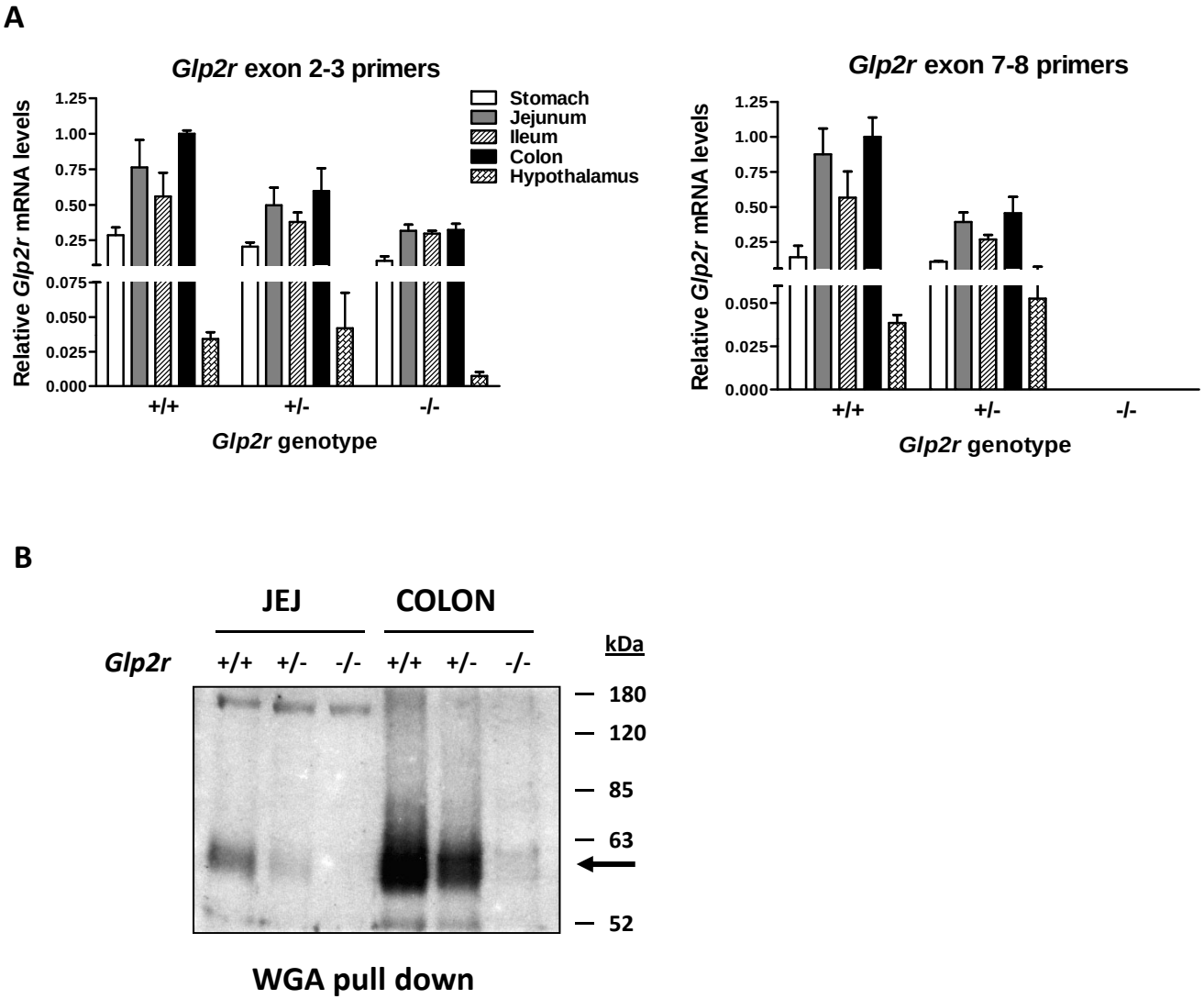

Supplementary Figure 4. *Glp2r expression in murine tissues.* (A) Quantitative Real Time PCR for exons 2-3 and 7-8 reveals absence of exons 7-8-containing *Glp2r* mRNA transcripts in stomach, jejunum, Ileum, colon and hypothalamus of *Glp2r*-/- mice (n=4 per group). (B) Representative Western blot analysis of immunoreactive GLP-2R protein (arrow, Mr ≅ 58 kDa) in wheat germ agglutinin (WGA)-purified tissue extracts from jejunum (JEJ) and colon of *Glp2r*+/+, +/- and -/- mice.

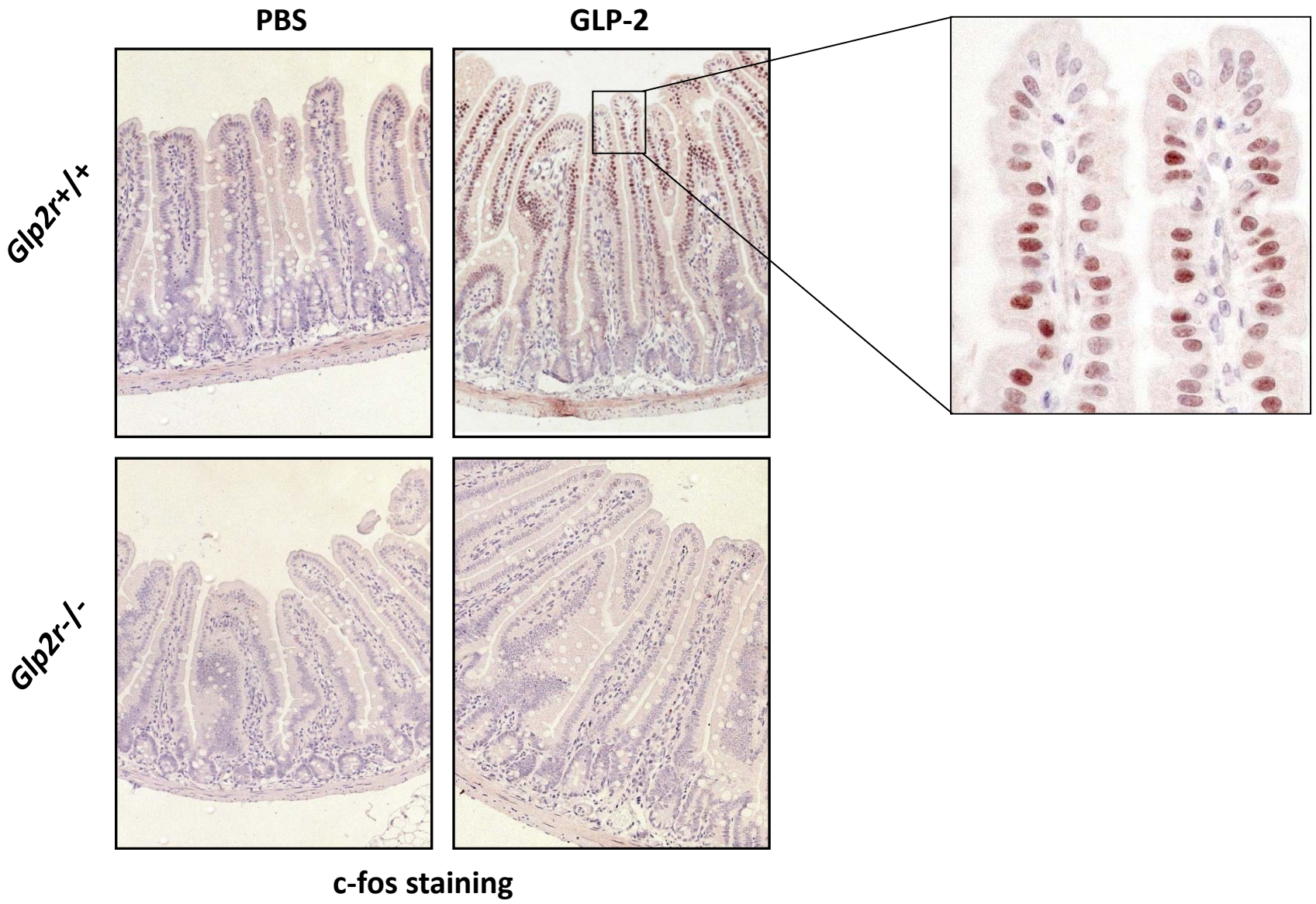

Supplementary Figure 5. Representative c-fos immunohistochemistry in jejunum of saline- and GLP-2-treated male *Glp2r*+/+ and *Glp2r*-/- mice 60 minutes after peptide administration.

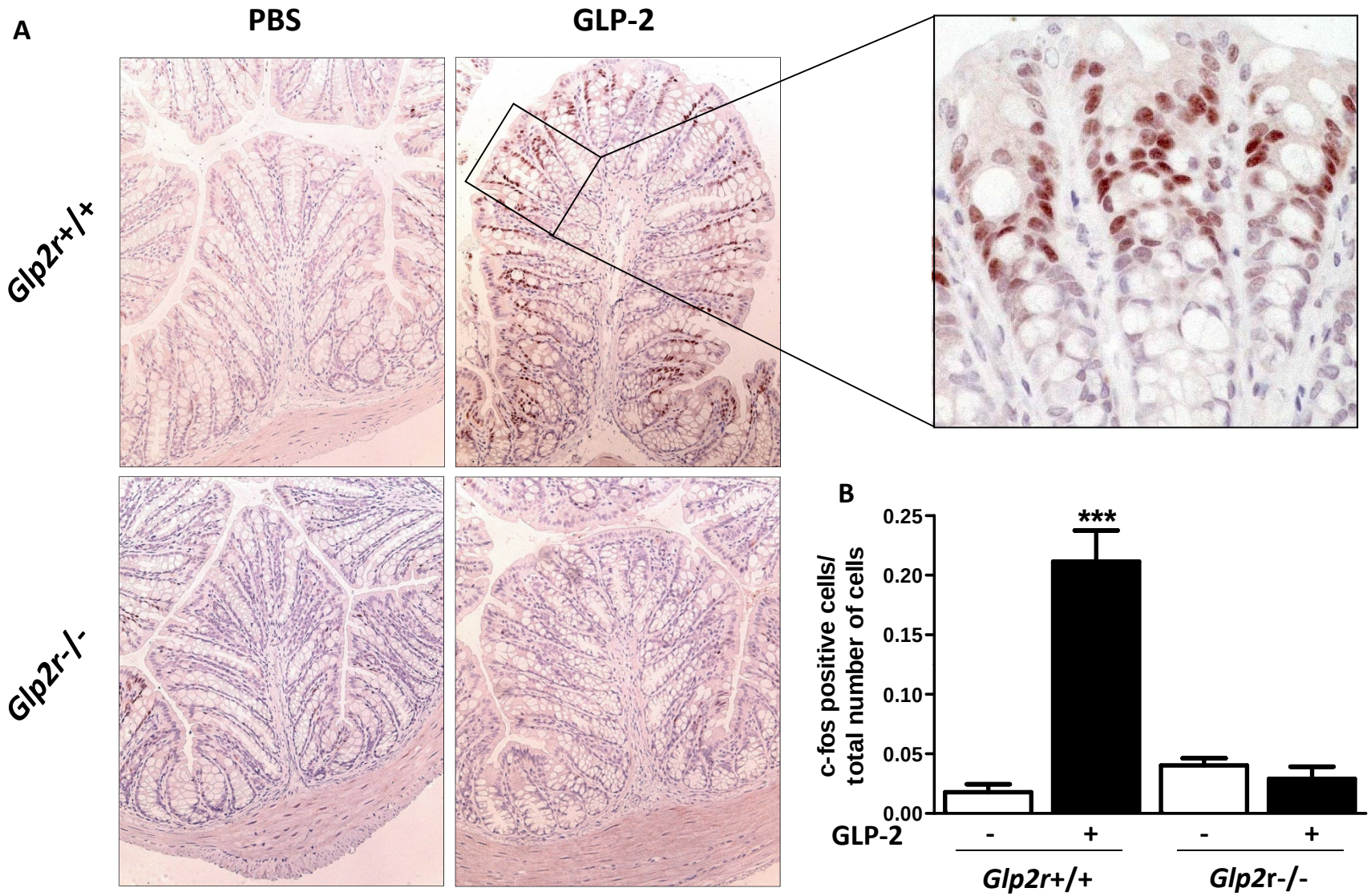

Supplementary Figure 6. (A) Representative c-fos immunohistochemistry in colonic epithelium of saline- and GLP-2-treated male *Glp2r*+/+ and *Glp2r*-/- mice 60 minutes after peptide administration. (B) Quantification of c-fos immunopositive nuclei (n = 3-4 mice). ***P<0.001 saline vs. GLP-2-treated mice.

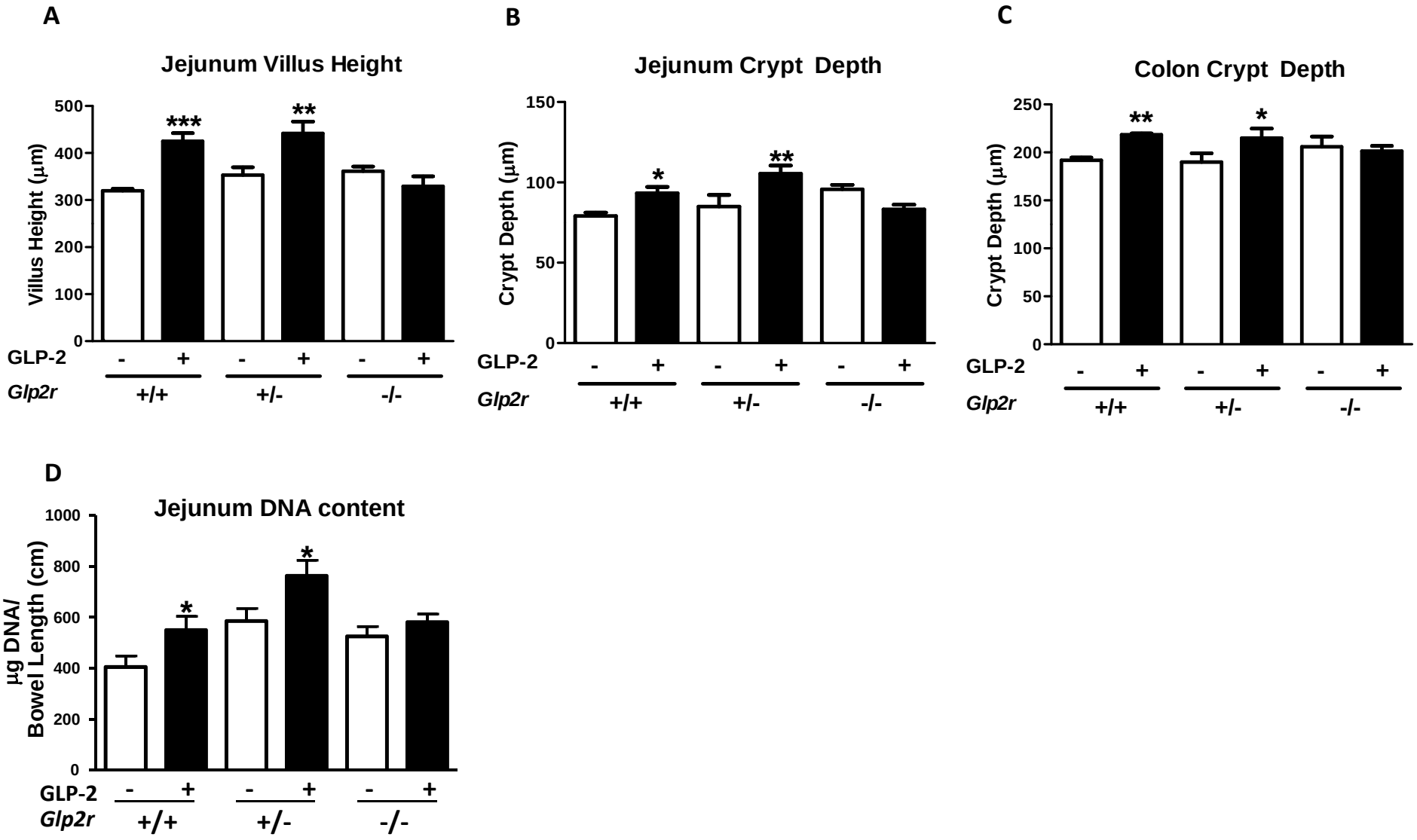

Supplementary Figure 7. (A) Jejunal villus height, (B) jejunal crypt depth, (C) colon crypt depth, and (D) jejunal DNA content in female *Glp2r+/+, Glp2r+/-* and *Glp2r-/-* mice treated with saline of GLP-2 (10 µg) once daily for 7 days (n=7-8 per group). *P<0.05, **P<0.01, ***P<0.001, saline vs. GLP-2-treated mice.

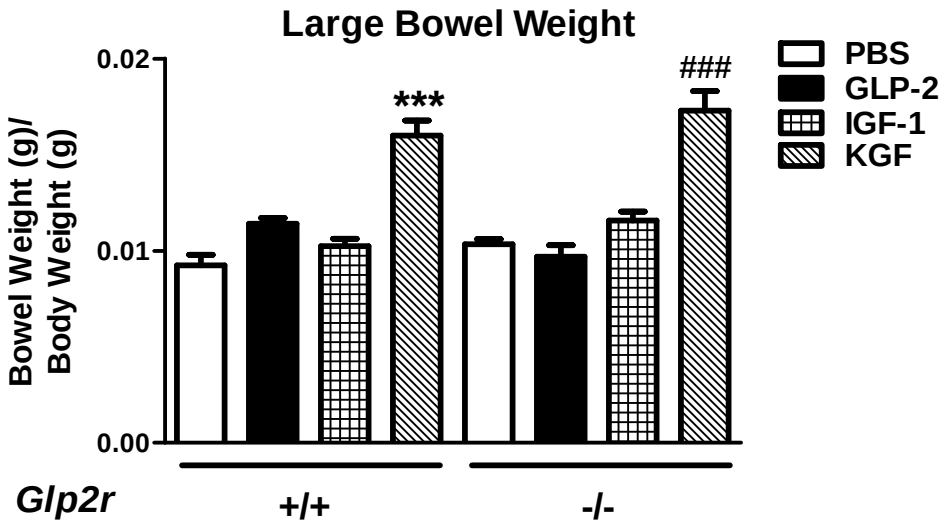

Supplementary Figure 8. *The large bowel of Glp2r-/- mice responds to exogenous KGF*. Human GLP-2 (2.5 μg twice daily), LongR3-insulin-like growth factor-1 (IGF-1; 25 μg twice daily) and recombinant human keratinocyte growth factor (KGF; 5 mg/kg once daily) were administered to female *Glp2r*+/+ and *Glp2r*-/- mice for 10 days prior to analysis of large bowel weight. ***p<0.001 vs saline-treated *Glp2r*+/+ mice. ### p<0.001 vs saline-treated *Glp2r*-/- mice (n=5-6 mice per group).

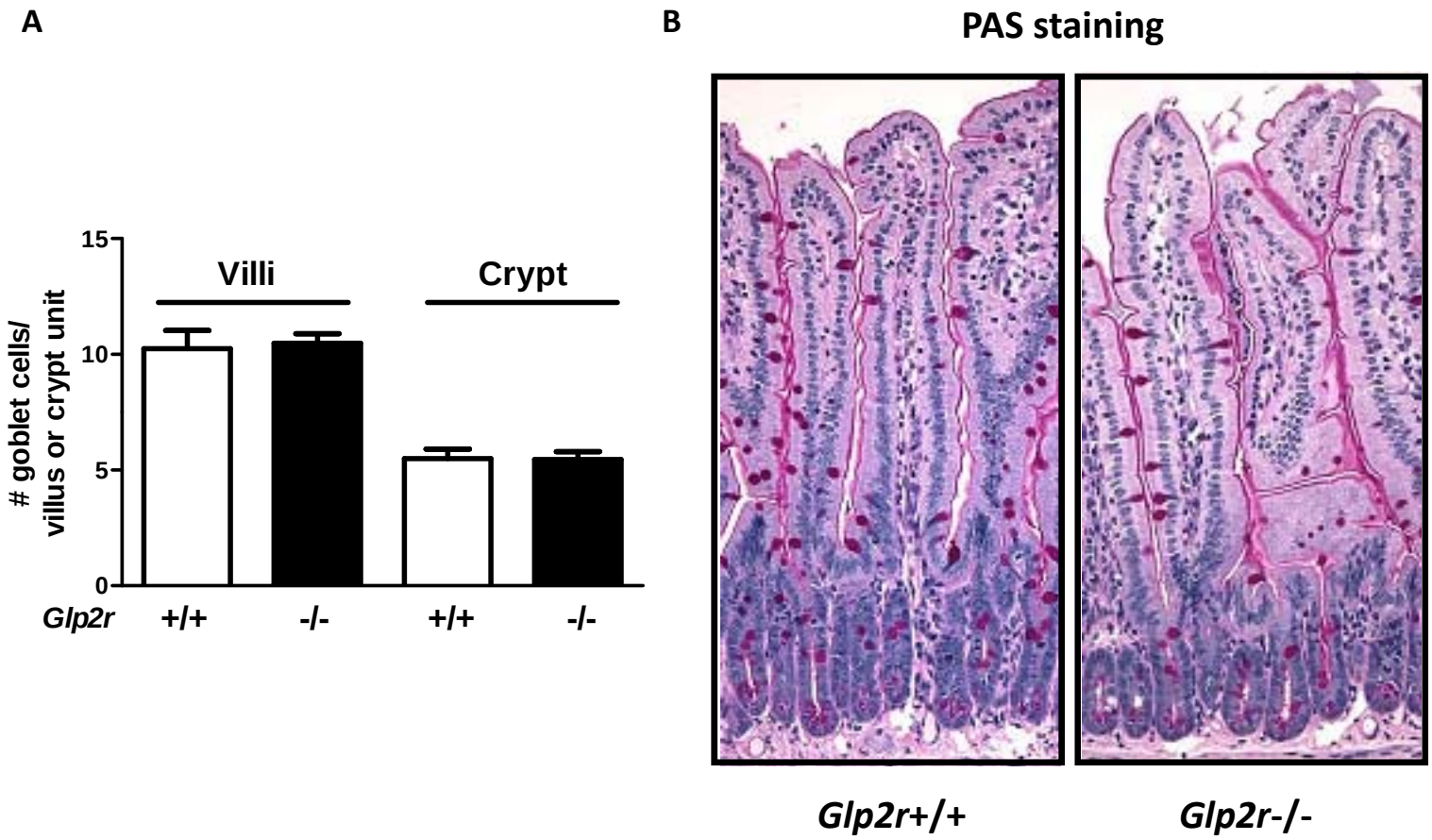

Supplementary Figure 9. (A) Quantification of PAS+ goblet cells in the small bowel villus and crypt compartments from male *Glp2r+/+* and *Glp2r-/-* mice (n=4 per group). (B) Representative PAS-stained jejunal histological sections.

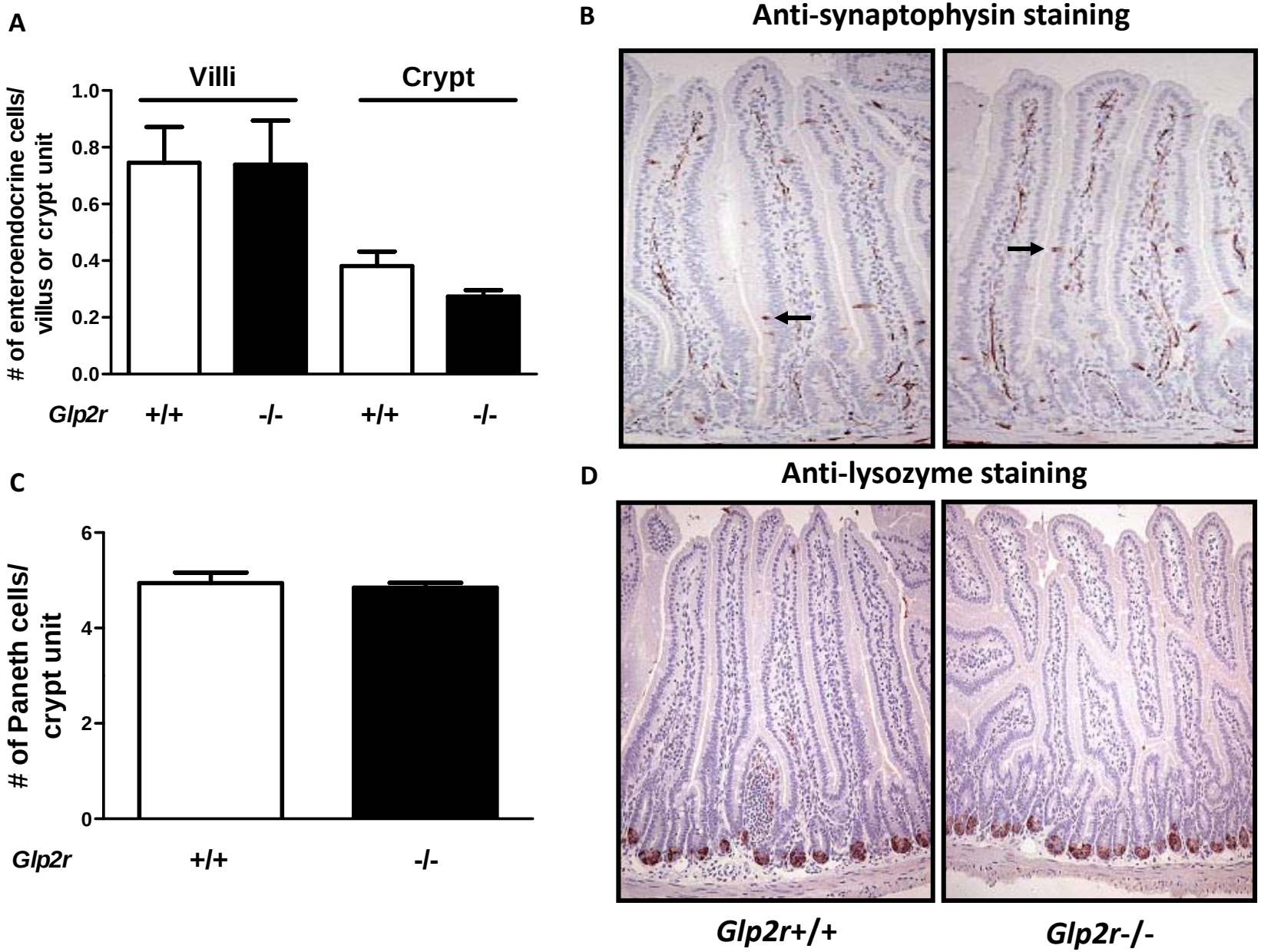

Supplementary Figure 10. Quantification of (A) enteroendocrine cells and (C) Paneth cells in the small bowel villus and crypt compartments from *Glp2r+/+* and *Glp2r-/-* mice (n=4 per group). Representative jejunal histological sections stained with (B) anti-synaptophysin and (D) anti-lysozyme antibodies to identify enteroendocrine (black arrows) and Paneth cells,respectively.